RAPID COMMUNICATIONS

PHYSICAL REVIEW C VOLUME 48, NUMBER 2 AUGUST 1993

Deformed intruder band in ^{113}I

E. S. Paul, C. W. Beausang, S. A. Forbes, S. J. Gale, A. N. James
P. M. Jones, and M. J. Joyce
Oliver Lodge Laboratory, University of Liverpool, P.O. Box 147, Liverpool L69 3BX, United Kingdom

R. M. Clark, K. Hauschild, I. M. Hibbert, and R. Wadsworth
Department of Physics, University of York, Heslington, York YO1 5DD, United Kingdom

R. A. Cunningham and J. Simpson
SERC Daresbury Laboratory, Daresbury, Warrington WA4 4AD, United Kingdom

T. Davinson, R. D. Page, P. J. Sellin, and P. J. Woods
Department of Physics, University of Edinburgh, Edinburgh EH9 3JZ, United Kingdom

D. B. Fossan, D. R. LaFosse, H. Schnare, and M. P. Waring
Department of Physics, State University of New York at Stony Brook, New York 11794

A. Gizon and J. Gizon
Institut des Sciences Nucléaires, Institut National de Physique Nucléaire et de Physique des Particules–Centre National de la Recherche Scientifique, Université Joseph Fourier, Grenoble, France

(Received 30 April 1993)

High-spin states in the neutron-deficient ^{113}I nucleus have been investigated for the first time using the ^{58}Ni(^{58}Ni,3$p\gamma$) reaction. Gamma-ray coincidence data were acquired with the Eurogam spectrometer in conjunction with the Daresbury recoil mass separator. A deformed intruder band has been established extending to a spin approaching 40$\hbar$ and excitation energy 30 MeV. A possible structure for the band is discussed. This is the first evidence for such a band in this mass region with Z>51.

PACS number(s): 21.10.Re, 27.70.+q, 23.20.Lv

Rotational structures in nuclei bordering on the spherical $Z = 50$ closed shell have been known for some time, e.g., Ref. [1]. Moreover, many well-deformed rotational cascades have recently been established to high spin in several odd-A antimony ($Z = 51$) isotopes [2,3]. This unexpected collectivity in these nuclei, which are essentially spherical in their ground states, is related to deformed 2-particle–2-hole $\pi[g_{7/2}^2 g_{9/2}^{-2}]$ 0_2^+ states in the even tin core nuclei. In addition, the strongly β-sloping $[550]1/2^-$ intruder orbital, from the $\pi h_{11/2}$ subshell above the $Z = 50$ shell gap, is thought to stabilize enhanced quadrupole deformed shapes analogous to the $[660]1/2^+$ intruder orbital for $A \sim 135$ nuclei [4]. In the odd-A iodine ($Z = 53$) isotopes, the low-lying yrast structures are explained by moderately deformed rotational bands based on the single $\pi h_{11/2}[550]1/2^-$ and $\pi g_{9/2}^{-1}[404]9/2^+$ Nilsson orbitals. In contrast to the antimony isotopes, the high-spin structure of the iodine isotopes is dominated by noncollective oblate structures, e.g., Refs. [5–7]. However, for ^{113}I a rotational cascade of 14 transitions extending to high spin ($I \sim 40\hbar$) and excitation energy ($\sim$30 MeV) has been found analogous to the antimony "intruder bands." This is the first example of such a structure for Z >51.

Prior to this work no information was available for states in ^{113}I. The present experiments involved the Eurogam [8,9] array coupled to the Daresbury recoil mass spectrometer [10] and employed the ^{58}Ni(^{58}Ni,3p)^{113}I reaction at a bombarding energy of 240 MeV. A preliminary experiment as part of Eurogam commissioning was performed for this reaction using 26 high efficiency ($\geq$70% relative to a 7.6 cm×7.6 cm NaI(Tl) crystal at 1.33 MeV) suppressed HPGe detectors in conjunction with the Daresbury recoil mass separator. Subsequently, a second experiment was performed using the full Eurogam array containing 45 HPGe detectors, again with the mass separator. For this second experiment, suppressed HPGe data were written to tape for events in which six or more "raw" (i.e., unsuppressed) HPGe's registered within a time coincidence window of 100 ns. A trigger rate of (2–3)×10^3 events per second was attained with the individual HPGe detectors counting at (6–7)×10^3 unsuppressed events per second. Recoil-γ events were also recorded when at least one HPGe registered. The recoil-γ rate was typically 2000 events per second. A total of 6×10^8 γ-γ events were unfolded from the high-fold (>3) γ-ray data.

A mass gated γ-γ matrix, containing $\sim$8×10^6 events, was constructed for A =113 in order to identify transitions in ^{113}I. Predictions from fusion evaporation codes show that the 3p channel into ^{113}I is the strongest exit channel for the ^{58}Ni + ^{58}Ni reaction at 240 MeV. In addition, these predictions indicate that neutron evaporation is extremely weak compared to charged particle emission. Hence the strong γ-ray transitions in the $A = 113$ matrix can be assigned to ^{113}I with some certainty. Furthermore, the ^{58}Ni + ^{58}Ni reaction has also recently been studied

at the TASCC (tandem accelerator superconducting cyclotron) facility of the Chalk River Laboratories of AECL Research, Canada, where charged-particle–γ-ray coincidences helped in the identification of the residual nuclei [11]. The deduced low-spin level structure for the new ^{113}I isotope (see Fig. 1) is also very similar to heavier odd-A I isotopes, e.g., ^{115}I [12]. Several γ-ray gated γ-γ matrices were subsequently constructed for ^{113}I from the triple- and higher-fold γ-ray events in order to build a level scheme. In addition, angular correlation information was obtained from the pure γ-ray coincidence data by sorting subsets of the data recorded by HPGe detectors at specific angles with respect to the beam axis. Matrices were constructed for groups of detectors at angles of 158° (5 detectors), 134° (10), and 86° (5) from which angular intensity ratios $I_\gamma(158°–158°)/I_\gamma(86°–158°)$ and $I_\gamma(134°–134°)/I_\gamma(86°–134°)$ could readily be extracted using spectra gated by transitions recorded by detectors at 158° and 134°, respectively. These intensity ratios were used to assist in the assignment of transition multipolarities using the method of directional correlation from oriented states (DCO) [13].

A partial level scheme of ^{113}I deduced from these experiments is shown in Fig. 1. A complete analysis of the low-lying structures will be presented in a forthcoming publication. The negative-parity band initiating on the $11/2^-$ state is identified with a band built on the $\pi h_{11/2}[550]1/2^-$ orbital, while the strongly coupled positive-parity band, shown to the lower left in Fig. 1, may be associated with the $\pi g_{9/2}^{-1}[404]9/2^+$ orbital. However, the present paper focuses on the band of fourteen stretched quadrupole transitions shown to the left in Fig. 1. Figure 2 shows a γ-ray spectrum, which represents the sum of double-gated spectra obtained from the pure γ-ray events. All transitions of the band, with the exception of the 949 keV and 2375 keV transitions, were used to construct this spectrum. The inset of Fig. 2 shows the sum of single gates set on the new band, obtained from the mass A =113 gated γ-γ matrix. The strong unlabeled transitions below 1 MeV form the yrast rotational band in Fig. 1 built on the $11/2^-$ state. The new band in ^{113}I is in coincidence with the negative-parity yrast levels with spin $35/2^-$ and below, in addition to the low-lying positive-parity band. The decay out of the band was not established but involves a second 1031 keV

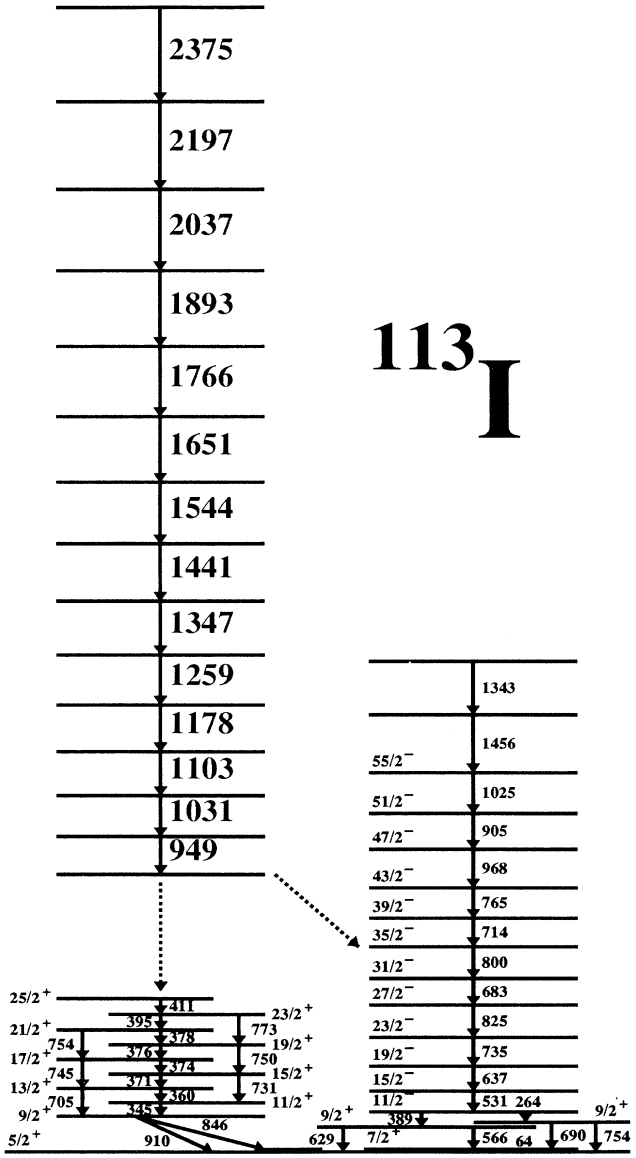

FIG. 1. Level scheme for ^{113}I deduced from this work. Transition energies are given in keV. The dashed transitions indicate where the intruder band feeds the low-spin structure.

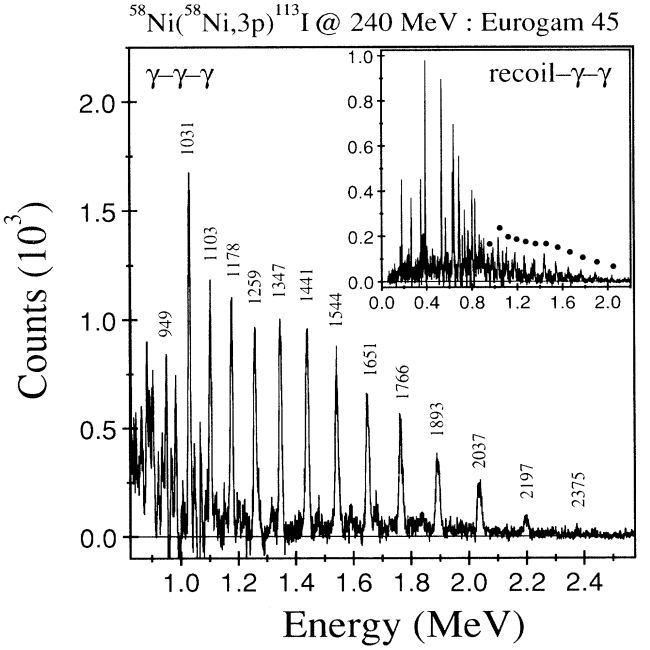

FIG. 2. Double-gated γ-ray spectrum showing transitions in the new intruder band in ^{113}I labeled in keV. The inset shows a mass selected (A=113) γ-ray spectrum gated by several of the band members. The positions of the band members are indicated by the solid circles, while the unlabeled lower energy transitions belong to the low spin yrast structure of ^{113}I.

transition plus a 1068 keV transition. The band is estimated to carry 2% of the intensity of the 531 keV $15/2^- \rightarrow 11/2^-$ transition, which itself carries in excess of 90% of the intensity in ^{113}I.

In order to assign a configuration to the band in ^{113}I, calculations have been performed using the total Routhian surface (TRS) cranking formalism (for details see, e.g., Ref. [4]). Results for configurations with specific parity and signature quantum numbers (π, α) are summarized in Fig. 3 which shows energies relative to a rigid-rotor reference plotted as a function of spin. The low spin $(-,-1/2)_1$ configuration with deformation parameters $(\beta_2 = 0.19, \gamma \sim +7°)$ may be associated with a band built on the $\pi h_{11/2}[550]1/2^-$ orbital and is identified with the negative-parity band initiating on the $11/2^-$ state in Fig. 1. The change of slope at $I \sim 18\hbar$ is related to the rotational alignment of a pair of low-Ω $h_{11/2}$ neutrons. Two other negative-parity configurations are seen at high spin. The $(-,-1/2)_2$ configuration has enhanced quadrupole deformation $(\beta_2 = 0.25, \gamma \sim +10°)$ while the high energy $(-,-1/2)_3$ configuration has a large quadrupole deformation with significant triaxiality $(\beta_2 = 0.36, \gamma \sim +25°)$. The microscopic structures for these configurations are presumably of the type $\pi[h_{11/2}g_{7/2}^2] \otimes \nu[h_{11/2}^m g_{7/2}^n]$ with m=2,4 and n= 2,0.

Positive-parity configurations are also shown in Fig. 3. The calculated deformation for the $(+,-1/2)_1$ configuration is $\beta_2 = 0.24, \gamma \sim +4°$ while the $(+,+1/2)_1$ configuration has deformation $\beta_2 = 0.26, \gamma \sim 0°$. The energy minimum for the latter positive-parity configuration is clearly seen for spins $28 < I < 43$ and is seen as yrast above $I = 35$ in Fig. 3 (dotted line). This spin range matches the estimated spins for the intruder band.

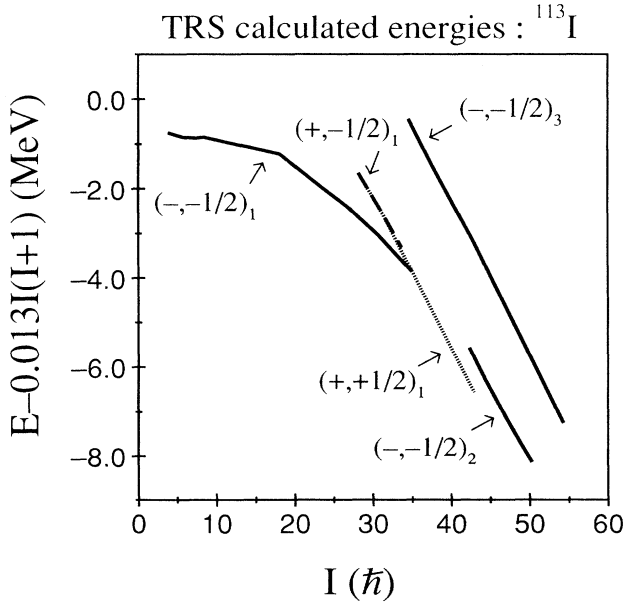

FIG. 3. TRS calculated energies, minus a rigid-rotor reference, plotted as a function of spin. Bands are classified by parity and signature (π, α) quantum numbers. It can be seen that the $(+,+1/2)_1$ configuration, with calculated deformation parameters $(\beta_2 = 0.26, \gamma \sim 0°)$, becomes yrast for $I > 35\hbar$.

The microscopic proton structure for the positive-parity configurations involves the $\pi[g_{7/2}h_{11/2}^2]$ and $\pi[d_{5/2}h_{11/2}^2]$ aligned protons, respectively, for the $(+,-1/2)_1$ and $(+,+1/2)_1$ configurations. The latter configuration involving the $\pi d_{5/2}[420]1/2^+$ orbital (which also represents the $5/2^+$ ground state of ^{113}I) allows the formation of the deformed $\pi[g_{7/2}^2 g_{9/2}^{-2}]_{0^+}$ 2-particle–2-hole state in the $Z = 50$ tin core. This deformed core state, together with the two rotationally aligned $h_{11/2}$ intruders, would indeed stabilize enhanced quadrupole deformation. At the high spins and frequencies observed for the band, rotationally aligned $h_{11/2}$ neutrons will also be present. Therefore, we propose an aligned $\pi[d_{5/2}h_{11/2}^2] \otimes \nu[h_{11/2}^2]$ configuration coupled to a deformed $\pi[g_{7/2}^2 g_{9/2}^{-2}]_{0^+}$ core state for the new intruder band in ^{113}I. This structure is different to the intruder bands in the antimony isotopes where only one $\pi h_{11/2}$ intruder is involved. With the higher proton Fermi surface for the iodine isotopes, the single $\pi h_{11/2}$ configuration already explains the moderately deformed $(\beta_2 \sim 0.18 - 0.20)$ yrast structures at low spin.

Cranked Woods-Saxon calculations have been performed for ^{113}I in order to corroborate the proposed intruder band structure. Deformation parameters $\beta_2 = 0.26$, $\gamma = 0°$ were used as suggested by the TRS calculations. The cranking calculations indicate the alignment of the $h_{11/2}$ neutron pair at a rotational frequency $\hbar\omega \sim 0.35$ MeV and the $h_{11/2}$ proton pair at $\hbar\omega \sim 0.50$ MeV. The latter frequency matches well the frequency at which the band depopulates (see Fig. 1, $E_\gamma \sim 1$ MeV and $\hbar\omega \approx E_\gamma/2$). Cranked Woods-Saxon calculations performed as a function of quadrupole deformation indicate an energy minimum for the $h_{11/2}$ neutrons at $\beta_2 \sim 0.23$ and at $\beta_2 \sim 0.38$ for the $h_{11/2}$ protons. It is thus the change in structure from $\pi[d_{5/2}] \otimes \nu[h_{11/2}^2]$ to $\pi[d_{5/2}h_{11/2}^2] \otimes \nu[h_{11/2}^2]$ at $\hbar\omega \sim 0.5$ MeV, associated with the occupation of the two $\pi h_{11/2}$ intruder orbitals, that may well induce and stabilize the enhanced deformation nature of the band. Similar effects are seen in the mass $A \sim 130$ region where, for example, in ^{132}Ce, the alignment of a pair of $\nu i_{13/2}$ intruder orbitals is able to induce the enhanced deformation $\beta_2 \sim 0.38$ [4]. Furthermore, depopulation of the band in ^{132}Ce is associated with the dealignment of the intruder pair, similar to the present case in ^{113}I.

Kinematic ($\mathcal{J}^{(1)} \sim I/\omega$, with assumed level spins) and dynamic ($\mathcal{J}^{(2)} \sim dI/d\omega$) moments of inertia for the new band in ^{113}I are shown in Fig. 4 together with the rigid-body estimate assuming a quadrupole deformation β_2=0.26. The dynamic moment of inertia of a similar intruder band in ^{109}Sb with a measured quadrupole deformation $\beta_2 \approx 0.20$ [14] is shown for comparison. The dynamic moment of inertia is higher in the case of ^{113}I, which may be related to larger deformation induced by the occupation of an extra $\pi h_{11/2}$ intruder; the ^{109}Sb band contains one $\pi h_{11/2}$ intruder while it is proposed that the ^{113}I band contains two $\pi h_{11/2}$ intruders. Given the proposed structure for the band in ^{113}I, the peak in the dynamic moment of inertia at $\hbar\omega \sim 0.52$ MeV can be related to the rotational alignment of the $\pi h_{11/2}$ intruders. The dynamic moment of inertia of the new

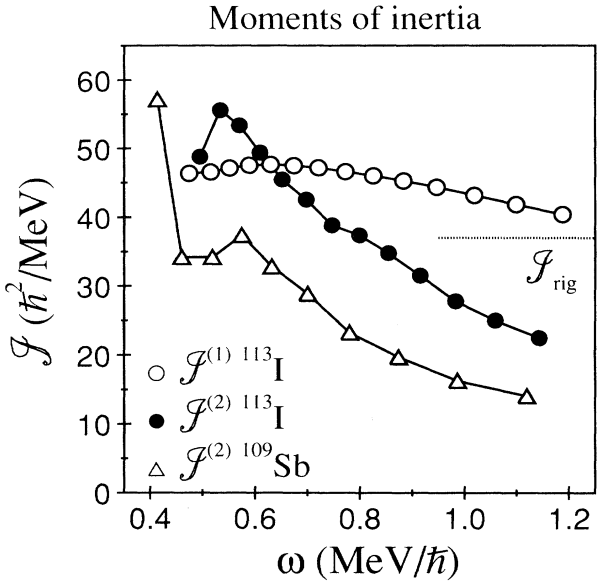

FIG. 4. Kinematic ($\mathcal{J}^{(1)} \sim I/\omega$) and dynamic ($\mathcal{J}^{(2)} \sim dI/d\omega$) moments of inertia for the new band in ^{113}I. Given the proposed configuration with $(\pi,\alpha)=(+,+1/2)$ as discussed in the text, a bandhead spin of 41/2 has been used in extracting the $\mathcal{J}^{(1)}$ moment of inertia. The dotted line represents the rigid-body estimate for a nucleus of mass A=113 with quadrupole deformation $\beta_2 = 0.26$. The dynamic moment of inertia of a similar band in ^{109}Sb is included for comparison.

band is seen to fall from 55 $\hbar^2\,\mathrm{MeV}^{-1}$ to 25 $\hbar^2\,\mathrm{MeV}^{-1}$ with increasing spin, while the kinematic moment of inertia is more constant, varying from 47 $\hbar^2\,\mathrm{MeV}^{-1}$ to 41 $\hbar^2\,\mathrm{MeV}^{-1}$ over the same frequency range. At high spin, therefore, $\mathcal{J}^{(1)} \sim 2\mathcal{J}^{(2)}$, and the difference in moments of inertia can be related to the contribution of single-particle angular momenta i_x aligned with the nuclear rotation axis. Values of $i_x \sim(15$–$20)\hbar$ are deduced at high spin, consistent with the proposed single-particle configuration for the intruder band. A significant component of the total spin is thus made up from single-particle angular momenta. Similar features are observed in ^{109}Sb [14] and ^{108}Sn [15], and may represent a novel form of "rotational" behavior at high spin.

The TRS calculations show the possibility for several near yrast configurations for well-deformed bands. Indeed, two or three weaker, less developed, intruder bands have been observed in the present data set, one of which can definitely be assigned to ^{112}Te from the mass-gated data. Analysis of the high-fold Eurogam data, together with the recoil-γ data will hopefully allow the other weaker structures to be assigned to specific nuclei.

In summary, a level scheme has been established for ^{113}I for the first time. At high spin, an "intruder" rotational band has been established. This is the first example of such a band in an iodine isotope, and extends the systematics of such structures in this mass region above $Z = 51$. A possible configuration, containing rotationally aligned $h_{11/2}$ proton and neutron pairs, has been suggested following TRS and Woods-Saxon cranking calculations.

The Eurogam project is funded jointly by the Science and Engineering Research Council (U.K.) and IN2P3 (France). This work was also partly funded by the National Science Foundation. Six of us (R.M.C., S.A.F., S.J.G., K.H., P.M.J., and M.J.J.) acknowledge the financial support of the SERC. We are indebted to Dr. R. Wyss and Dr. W. Nazarewicz for providing the TRS and Woods-Saxon cranking codes. Finally, the numerous people involved in the operation of the Eurogam array at Daresbury are thanked, together with the accelerator staff.

[1] J. Bron, W.H.A. Hesselink, A. van Poelgeest, J.J.A. Zalmstra, M.J. Uitzinger, H. Verheul, K. Heyde, M. Waroquier, H. Vincx, and P. van Isacker, Nucl. Phys. **A318**, 335 (1979).

[2] D.R. LaFosse, D.B. Fossan, J.R. Hughes, Y. Liang, P.Vaska, M.P. Waring, and J.-y. Zhang, Phys. Rev. Lett. **69**, 1332 (1992).

[3] V.P. Janzen, H.R. Andrews, B. Haas, D.C. Radford, D. Ward, A. Omar, D. Prévost, M. Sawicki, P. Unrau, J.C. Waddington, T.E. Drake, A. Galindo-Uribarri, and R. Wyss, Phys. Rev. Lett. **70**, 1065 (1993).

[4] R. Wyss, J. Nyberg, A. Johnson, R. Bengtsson, and W. Nazarewicz, Phys. Lett. B **215** 211 (1988).

[5] Y. Liang, D.B. Fossan, J.R. Hughes, D.R. LaFosse, T. Lauritsen, R. Ma, E.S. Paul, P. Vaska, M.P. Waring, N. Xu, and R.A. Wyss, Phys. Rev. C **44**, R578 (1991).

[6] E.S. Paul, J. Simpson, H. Timmers, I. Ali, M.A. Bentley, A.M. Bruce, D.M. Cullen, P. Fallon, and F. Hanna, J. Phys. G **18**, 971 (1992).

[7] E.S. Paul, J. Simpson, S. Araddad, C.W. Beausang, M.A. Bentley, M.J. Joyce, and J.F. Sharpey-Schafer, J. Phys. G **19**, 913 (1993).

[8] C.W. Beausang, S.A. Forbes, P. Fallon, P.J. Nolan, P.J. Twin, J.N. Mo, J.C. Lisle, M.A. Bentley, J. Simpson, F.A. Beck, D. Curien, G. deFrance, and G. Duchêne, Nucl. Instrum. Methods **A313** 37 (1992).

[9] P.J. Nolan, Nucl. Phys. **A520** 657c (1990).

[10] A.N. James, T.P. Morrison, K.L. Ying, K.A. Connell, H.G. Price, and J. Simpson, Nucl. Instrum. Methods **A267** 144 (1988).

[11] V.P. Janzen, private communication (1992).

[12] E.S. Paul, R.M. Clark, S.A. Forbes, D.B. Fossan, J.R. Hughes, D.R. LaFosse, Y. Liang, R. Ma, P.J. Nolan, P.H. Regan, P. Vaska, R. Wadsworth, and M.P. Waring, J. Phys. G **18**, 837 (1992).

[13] K.S. Krane, R.M. Steffen, and R.M. Wheeler, Nucl. Data Tables **A11** 351 (1973).

[14] V.P. Janzen, D.R. LaFosse, H. Schnare, D.B. Fossan, A. Galindo-Uribarri, S.M. Mullins, E.S. Paul, L. Persson, S. Pilotte, D.C. Radford, H. Timmers, J.C. Waddington, R. Wadsworth, D. Ward, J.N. Wilson, and R. Wyss, submitted to Phys. Rev. Lett.

[15] R. Wadsworth, H.R. Andrews, R.M. Clark, D.B. Fossan, A. Galindo-Uribarri, V.P. Janzen, J.R. Hughes, D.R. LaFosse, S.M. Mullins, E.S. Paul, D.C. Radford, P. Vaska, M.P. Waring, D. Ward, J.N. Wilson, and R. Wyss, Nucl. Phys. A (in press).